

# New results on the Roper resonance and the $P_{11}$ partial wave

A.V. Sarantsev<sup>a,b</sup>, M. Fuchs<sup>a</sup>, M. Kotulla<sup>c,d</sup>, U. Thoma<sup>a,d</sup>,  
 J. Ahrens<sup>e</sup>, J.R.M. Annand<sup>f</sup>, A.V. Anisovich<sup>a,b</sup>, G. Anton<sup>g</sup>,  
 R. Bantes<sup>h</sup>, O. Bartholomy<sup>a</sup>, R. Beck<sup>a,e</sup>, Yu. Beloglazov<sup>b</sup>,  
 R. Castelijns<sup>i</sup>, V. Crede<sup>a,j</sup>, A. Ehmans<sup>a</sup>, J. Ernst<sup>a</sup>, I. Fabry<sup>a</sup>,  
 H. Flemming<sup>k</sup>, A. Fösel<sup>g</sup>, Chr. Funke<sup>a</sup>, R. Gothe<sup>h</sup>,  
 A. Gridnev<sup>b</sup>, E. Gutz<sup>a</sup>, St. Höffgen<sup>h</sup>, I. Horn<sup>a</sup>, J. Höbl<sup>g</sup>,  
 D. Hornidge<sup>e</sup>, S. Janssen<sup>d</sup>, J. Junkersfeld<sup>a</sup>, H. Kalinowsky<sup>a</sup>,  
 F. Klein<sup>h</sup>, E. Klempt<sup>a</sup>, H. Koch<sup>k</sup>, M. Konrad<sup>h</sup>, B. Kopf<sup>k</sup>,  
 B. Krusche<sup>c</sup>, J. Langheinrich<sup>h</sup>, H. Löhner<sup>i</sup>, I. Lopatin<sup>b</sup>,  
 J. Lotz<sup>a</sup>, J.C. McGeorge<sup>f</sup>, I.J.D. MacGregor<sup>f</sup>, H. Matthäy<sup>k</sup>,  
 D. Menze<sup>h</sup>, J.G. Messchendorp<sup>d,i</sup>, V. Metag<sup>d</sup>, V.A. Nikonov<sup>a,b</sup>,  
 D. Novinski<sup>b</sup>, R. Novotny<sup>d</sup>, M. Ostrick<sup>h</sup>, H. van Pee<sup>a</sup>,  
 M. Pfeiffer<sup>d</sup>, A. Radkov<sup>b</sup>, G. Rosner<sup>f</sup>, M. Rost<sup>e</sup>, C. Schmidt<sup>a</sup>,  
 B. Schoch<sup>h</sup>, G. Suft<sup>g</sup>, V. Sumachev<sup>b</sup>, T. Szczepanek<sup>a</sup>,  
 D. Walther<sup>h</sup>, D.P. Watts<sup>f</sup>, and Chr. Weinheimer<sup>a</sup>

<sup>a</sup>*Helmholtz-Institut für Strahlen- und Kernphysik der Universität Bonn, Germany*

<sup>b</sup>*Petersburg Nuclear Physics Institute, Gatchina, Russia*

<sup>c</sup>*Physikalisches Institut, Universität Basel, Switzerland*

<sup>d</sup>*II. Physikalisches Institut, Universität Giessen*

<sup>e</sup>*Institut für Kernphysik, Universität Mainz, Germany*

<sup>f</sup>*Department of Physics and Astronomy, University of Glasgow, UK*

<sup>g</sup>*Physikalisches Institut, Universität Erlangen, Germany*

<sup>h</sup>*Physikalisches Institut, Universität Bonn, Germany*

<sup>i</sup>*KVI, Groningen, Netherlands*

<sup>j</sup>*Department of Physics, Florida State University, USA*

<sup>k</sup>*Physikalisches Institut, Universität Bochum, Germany*

---

**Abstract**

Properties of the Roper resonance, the first scalar excitation of the nucleon, are determined. Pole positions and residues of the  $P_{11}$  partial wave are studied in a combined analysis of pion- and photo-induced reactions. We find the Roper pole at  $\{(1371 \pm 7) - i(92 \pm 10)\}$  MeV and an elasticity of  $0.61 \pm 0.03$ . The largest decay coupling is found for the  $N\sigma$  ( $\sigma = (\pi\pi)$ - $S$ -wave). The analysis is based on new data on  $\gamma p \rightarrow p\pi^0\pi^0$  for photons in the energy range from the two-pion threshold to 820 MeV from TAPS at Mainz and from 0.4 to 1.3 GeV from Crystal Barrel at Bonn and includes further data from other experiments. The partial wave analysis excludes the possibility that the Roper resonance is split into two states with different partial decay widths.

*PACS: 11.80.Et, 13.30.-a, 13.40.-f, 13.60.Le*

---

The lowest-mass excitation of the nucleon, the Roper  $N(1440)P_{11}$  resonance with spin and parity  $J^P = 1/2^+$ , and the second scalar nucleon excitation  $N(1710)P_{11}$  [1], remain to be the most enigmatic states in baryon spectroscopy. In the bag model [2] and in the Skyrme model [3], the Roper resonance was interpreted as surface oscillation, also called breathing mode. In quark models, two low-mass scalar excitations of the nucleon are predicted. Using a linear confining potential and one-gluon-exchange [4] or instanton-induced interactions [5], a level ordering is calculated in which the mass of the  $N(1440)P_{11}$  exceeds the mass of the negative-parity state  $N(1535)S_{11}$  by 80 MeV; experiments find it  $\sim 100$  MeV below. The spacing between the two scalar excitations is predicted to be  $\sim 220$  MeV [4,5,6] while experiments find 270 MeV [1]. When one-gluon exchange interactions are replaced by exchanges of Goldstone bosons, the  $N(1440)P_{11}$  mass can well be reproduced [7], the  $N(1710)P_{11}$  mass was not calculated. Lattice gauge calculations indicate that the first scalar excitation of the nucleon should be expected above  $N(1535)S_{11}$  [8]. Compared to model and lattice predictions, the mass of the Roper resonance is too small; compared to other low-mass resonances, its width too large.

These problems would not occur if  $N(1710)P_{11}$  were the first radial scalar excitation of the proton. The Roper resonance can then be interpreted within a coupled-channel meson exchange model based on an effective chiral-symmetric Lagrangian [9]; no genuine  $N(1440)$  (3 quark) resonance was needed to fit  $\pi N$  phase shifts and inelasticities, in agreement with [10]. Motivated by the  $Q^2$  dependence of the Roper helicity amplitude which would seem to suggest a hybrid nature [11], Capstick and Page [12] calculated masses of baryonic hybrids. Their masses were, however, too large to interpret the Roper resonance as a hybrid. The  $\Theta^+(1530)$ , a baryon with positive strangeness, which may have been observed in low-statistics photo-production experiments [13,14,15,16], made the Roper resonance [17] and/or the  $N(1710)P_{11}$  [18] to viable pentaquark

candidates. The existence of a very narrow  $P_{11}$  state in the mass region 1650–1750 MeV was investigated in [19]. The fading evidence for  $\Theta^+(1530)$  [20,21] makes this interpretation less attractive. Morsch and Zupranski [22] suggested the Roper mass region might house two resonances, one at 1390 MeV with a small elastic width and large coupling to  $N\pi\pi$ , and a second one at higher mass – around 1460 MeV – with a large elastic width and small  $N\pi\pi$  coupling. The former resonance was found to be produced in  $\pi N$  scattering, and in  $\alpha$ -proton scattering using an  $\alpha$  beam of  $E_\alpha = 4.2$  GeV kinetic energy; the latter resonance was suggested to be excited by  $\gamma N$ . The two resonances may have rather different wave functions [23]. Studies of the reaction  $pp \rightarrow pp\pi^+\pi^-$  suggested that the low-energy tail of the Roper resonance might decay to both  $N\sigma$  and  $\Delta\pi$  [24]. Obviously, the  $P_{11}$  partial wave is not sufficiently constrained by precision data and supports very different interpretations.

In this letter, we present data on  $\gamma p \rightarrow p\pi^0\pi^0$  of the A2-TAPS collaboration at the Mainz Microtron (MAMI) electron accelerator [25] and of the CB-ELSA collaboration at the Bonn ELectron Stretcher Accelerator (ELSA) [26]. The Bonn set up and the analysis method was described briefly in the preceding paper [27]. Here we give only a short summary of the TAPS setup, for more details see [28]. Earlier data taken at MAMI [29,30] have smaller statistics and are not discussed here.

The photon energy at MAMI covered the range 285–820 MeV. The photon energies were measured in the Glasgow tagged photon facility [31] with an average energy resolution of 2 MeV. The TAPS detector [32,33] consisted of six blocks each with 62 hexagonally shaped BaF<sub>2</sub> crystals arranged in an 8×8 matrix and a forward wall with 138 BaF<sub>2</sub> crystals arranged in a 11×14 rectangle. This setup covered  $\approx 40\%$  of  $4\pi$ . The  $\gamma p \rightarrow \pi^0\pi^0 p$  reaction channel was identified by constructing the 4-momenta of the two neutral pions from their  $\gamma\gamma$  decays; proton detection was not required in the analysis. The  $\pi^0$  mesons were detected via their  $2\gamma$  decay and identified by their invariant mass. The mass of the missing particle was calculated from the four-momenta of the pions, and the beam energy  $E_\gamma$  using the mass of the target proton. The resulting distribution is shown in Fig. 1a and demonstrates the unambiguous identification of the reaction  $\gamma p \rightarrow \pi^0\pi^0 p$ . At incident beam energies above the  $\eta$  production threshold of  $E_\gamma = 707$  MeV, a possible background from the  $\eta \rightarrow 3\pi^0$  decay with one undetected  $\pi^0$  can be cleanly separated from the reaction of interest (see Fig. 1a). Further details are given in [34].

In Fig. 1b the total cross section is displayed. Two peaks due to the second and third resonance region are observed, with peaks at  $\sim 1500$  and  $\sim 1700$  MeV. There is good general agreement between the three data sets. The GRAAL data [35] fall off at high masses more rapidly than the CB-ELSA data. At low energies, the TAPS data fall below the CB-ELSA data while the peak cross sections of all 3 experiments agree reasonably well. The discrepancies

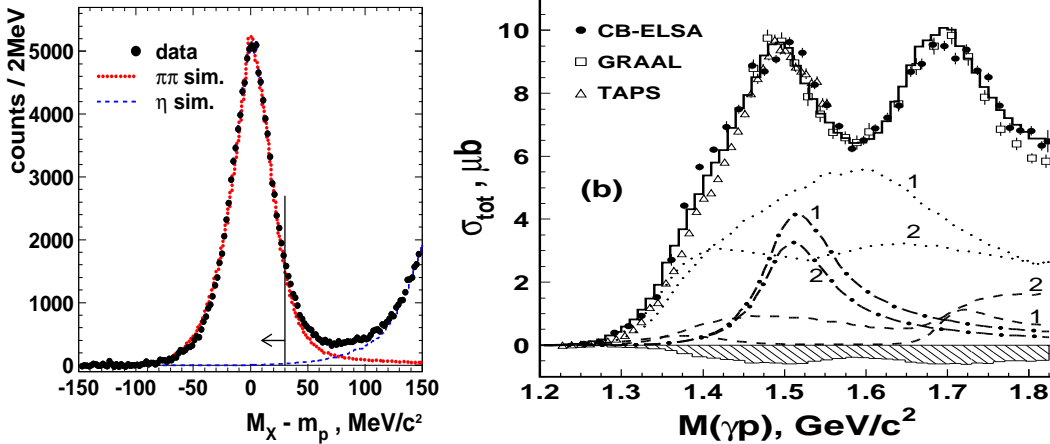


Fig. 1. a) TAPS: Missing mass  $M_X - m_p$  calculated from two detected  $\pi^0$  mesons for incident beam energies  $E_\gamma \leq 820$  MeV (data: symbols with errors,  $\pi^0\pi^0$  simulation dotted line,  $\eta$  simulation dashed line). The cut to eliminate  $\eta$  background is indicated. b) Total cross sections for  $\gamma p \rightarrow p\pi^0\pi^0$ . The shaded area below the zero line represents the systematic error of the CB-ELSA data, the solid line a PWA fit. There are two PWA solutions, marked 1 and 2, giving a similar likelihood (see text). The  $D_{33}$  partial wave (dotted line) gives the strongest contribution to the second resonance region, followed by  $D_{13}$  (dashed-dotted line) and  $P_{11}$  (dashed line). The  $D_{13} - D_{33}$  interference generates the dip between the second and third resonance region.

show the difficulties of extracting total cross sections when the full phase space is not covered by the detector. Note that the extrapolation was done differently: the CB-ELSA and the A2-TAPS collaborations used the result of this partial wave analysis; the GRAAL collaboration used a simulation based on  $\gamma p \rightarrow \Delta^+\pi^0$  and  $\gamma p \rightarrow p\pi^0\pi^0$  phase space. The inclusion of both, CB-ELSA and TAPS data, provides an additional tool to estimate the systematic error of the experimental data. The fit curves in Fig. 1b are discussed below.

The total cross section gives only a very superficial view of the reaction. Fig. 2a shows the experimental  $p\pi^0\pi^0$  Dalitz plots, Fig. 2b,c the  $p\pi^0$  and  $\pi^0\pi^0$  mass distributions. The solid line represents the result of a fit, the dashed line represents the distribution of reconstructed phase space events. The projections are not corrected for detection efficiency to allow the reader to compare data and fit directly. From the  $\pi^0 p$  mass distributions we conclude that the  $\Delta$  isobar plays an important role in the two-pion photoproduction dynamics. The  $\pi^0\pi^0$  mass distributions are featureless but show strong deviations from phase space.

Even the Dalitz plot and the projections do not carry the full information on the reaction dynamics. The full sensitivity of the data can only be exploited using an event-based likelihood fit. The data presented here were subjected to a partial wave analysis based on the Bonn-Gatchina approach [36,37]. Com-

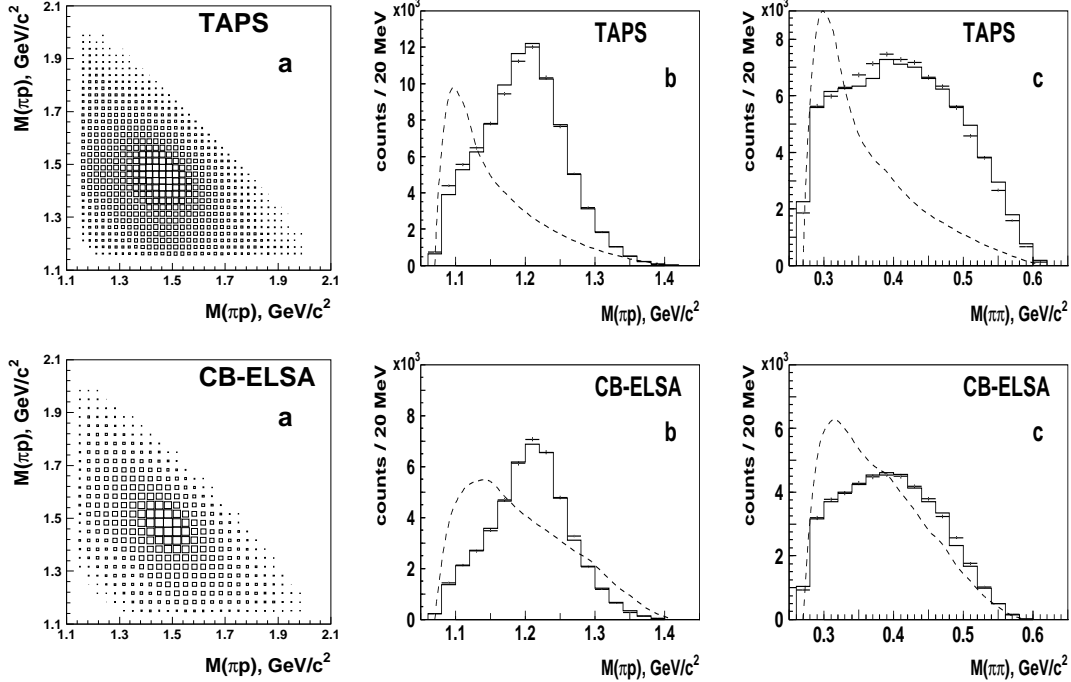


Fig. 2. Dalitz plots (a) and  $p\pi^0$  (b) and  $\pi^0\pi^0$  (c) mass distributions for TAPS (upper row) and for CB-ELSA (lower row) data for  $\gamma p \rightarrow p\pi^0\pi^0$ . The CB-ELSA data shown here are restricted to  $M \leq 1.55$  GeV. In (b,c), data are represented by crosses, the fit as histogram. The dashed lines represents the phase space contributions within the acceptance. The distributions are not corrected for acceptance which are different for the two experiments, leading to different distributions.

pared to a previous analysis [38,39], several new data sets are included in this analysis. A list of additional data and a description of the partial wave analysis method can be found in [40]. In the case of two-particle final states (including  $\gamma p \rightarrow \Lambda K^+$  and  $\gamma p \rightarrow \Sigma K$ ), angular distributions are fitted; three-body final states like  $N\pi^0\pi^0$  and  $p\pi^0\eta$  [41] undergo an event-based likelihood fit.

The reactions most relevant for the present analysis are collected in Table 1. The  $\pi N$  elastic scattering [46] amplitude provides a strong constraint for  $N\pi$  partial decay widths of resonances in this partial wave. The inclusion of data on  $\gamma p \rightarrow p\pi^0$  [42,43,44,45] and on  $\pi^- p \rightarrow n\pi^0\pi^0$  [47] over-constrains resonance properties: the three partial decay widths,  $\Gamma_{N\gamma}$ ,  $\Gamma_{N\pi}$ , and  $\Gamma_{N\pi\pi}$ , of the Roper

Table 1

The reactions most important for the study of properties of the Roper resonance.

1	$\gamma p \rightarrow p\pi^0\pi^0$	Figs. 1,2	this work
2	$\gamma p \rightarrow p\pi^0$	Figs. 3-5	[42,43,44,45]
3	$\pi N \rightarrow N\pi$	Fig. 6	[46]
4	$\pi^- p \rightarrow n\pi^0\pi^0$	Fig. 7	[47]

$N(1440)P_{11}$  resonance have to describe its properties in four reactions. In addition, the partial widths define the number of events ascribed to the Roper resonance in the reactions above. Their sum must equal the total width since the only missing channel,  $N(1440)P_{11} \rightarrow N\rho$ , is expected to provide a very small contribution due to the small available phase space. We believe that the tight constraints due to the use of four different reactions defines the Roper mass, width, and coupling constants with much higher reliability than analyses of individual reactions can do. The background amplitudes in the four reactions are treated independently. The data and the quality of the description are shown in Figs. 1-7.

We started the partial wave analysis from the solution given in [38,39]. Including the new data, we found good compatibility for masses and widths of the contributing resonances. The new description of single  $\pi^0$  photoproduction is shown in Fig. 3. In Figs. 4 and 5 we present a comparison of fit and data on target asymmetry and on the proton recoil polarization from different experiments [48]. Inclusion of the latter data had an impact on the size of couplings but did not change the pole positions; the properties of the Roper resonance were nearly unaffected. The figures (not the fits) are restricted to the mass range below 1800 MeV.

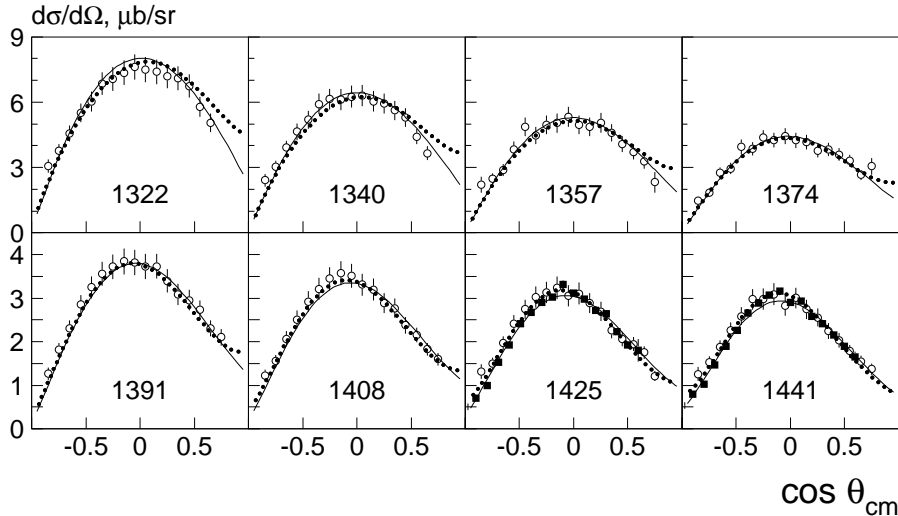


Fig. 3. The  $\gamma p \rightarrow p\pi^0$  differential cross section. Open circles [42]; full circles:[44] . Solid lines: our fit; dotted lines: SAID, the solution FA06 [45].

The  $\gamma p \rightarrow p\pi^0\pi^0$  data provide new information on the  $N\pi\pi$  decay modes. The  $D_{33}$  amplitude gives the largest contribution to this data (see Fig. 1b). Its interference with  $N(1520)D_{13}$ , constructive at  $\sim 1500$  MeV, destructive at  $\sim 1600$  MeV, generates the dip between the two peaks in the total cross section. The  $\Delta(1700)D_{33}$  has a large coupling to  $\Delta\pi$ . In the main solution,  $\Delta(1700)D_{33}$  decays into  $\Delta\pi$  in a relative  $S$  wave. There is however a second solution with very similar likelihood in which the  $\Delta(1700)D_{33} \rightarrow \Delta\pi$  decays proceed via

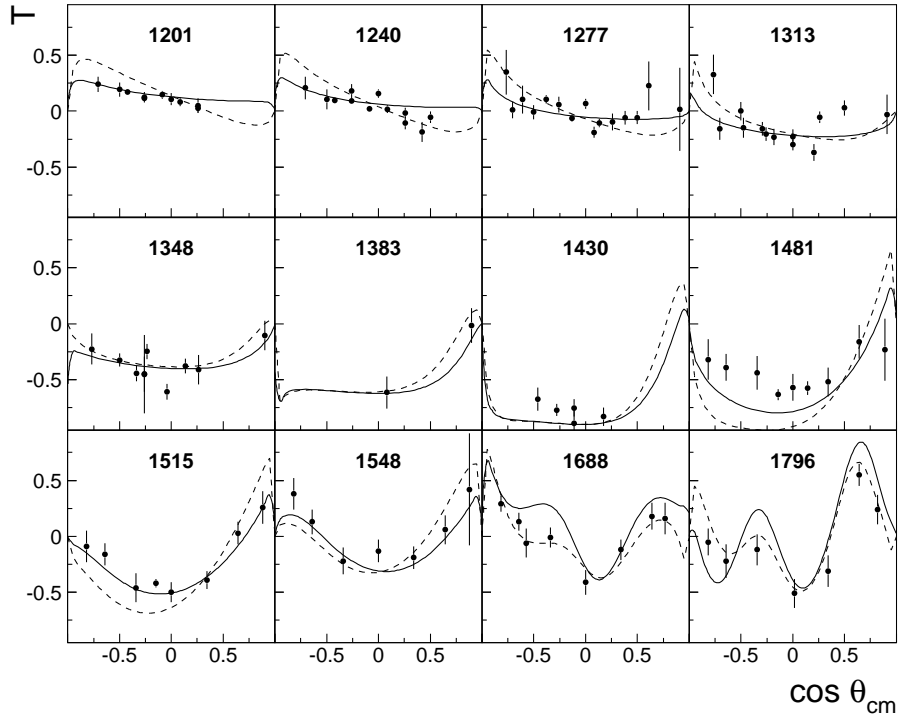


Fig. 4. The target asymmetry from different experiments [48] for selected 5 MeV mass bins. Solid lines: our fit; dashed lines: SAID, the solution FA06 [45].

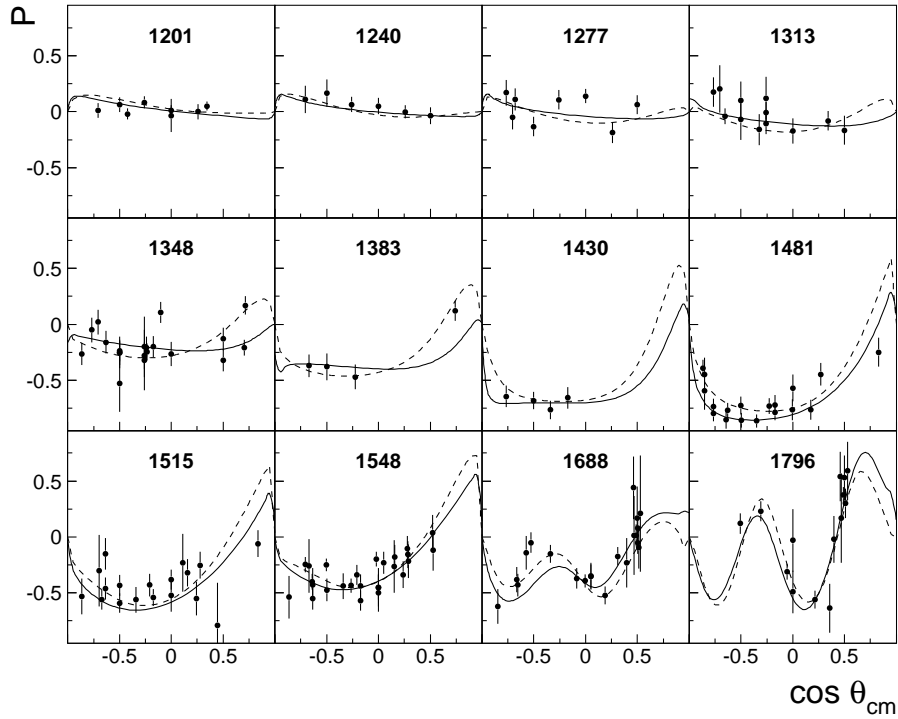


Fig. 5. The proton recoil polarization from different experiments [48] for selected 5 MeV mass bins. Solid lines: our fit; dashed lines: SAID, the solution FA06 [45].

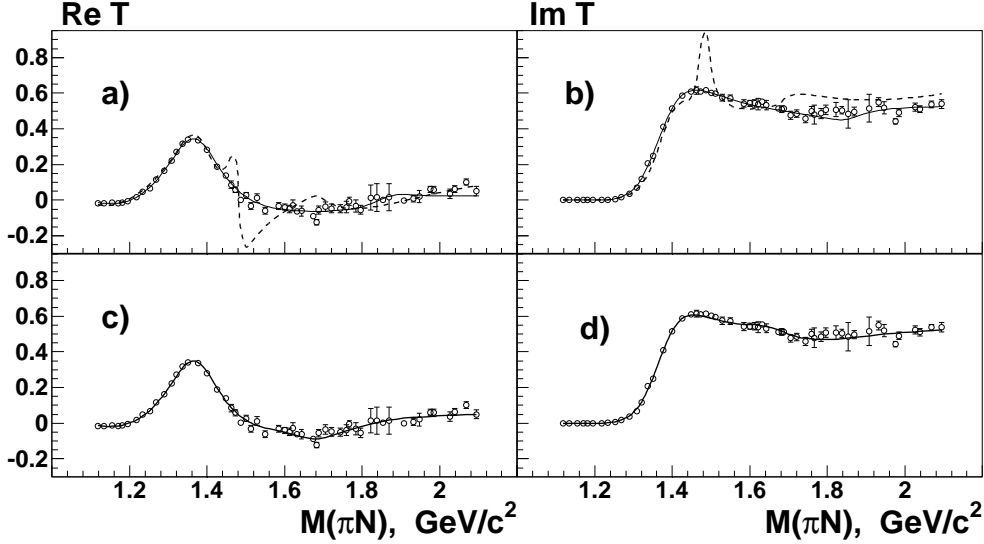


Fig. 6. Real (a,c) and imaginary (b,d) part of the  $\pi N$   $P_{11}$  elastic scattering amplitude; data and fit with two (a,b) and three (c,d) poles [46]. The dashed line in (a,b) represents a fit in which the Roper resonance is split into two components. The overall likelihood deteriorates to extremely bad values. The fit tries to make one Roper resonance as narrow as possible.

$D$ -wave. This ambiguity results in different contributions of all  $p\pi^0\pi^0$  partial waves as shown in Fig. 1b. The interference between  $\Delta(1700)D_{33}$  and background contributions is responsible for the shallow dent in solution 2 of the  $D_{33}$  contribution visible in Fig. 1b.

The importance of the  $(\pi\pi)$ - $S$ -wave was already hinted at by Murphy and Laget (quoted by the GRAAL collaboration in [35]), although in a very different framework based on an effective isobaric Lagrangian. In the Laget model, the Roper resonance provided the largest contribution to  $N\pi\pi$ , followed by the  $D_{13}$  partial wave while  $D_{33}(1700)$  was very weak. The Valencia model [49,50] is limited to  $E_\gamma < 0.84$  GeV; it predicted strong contributions of  $D_{13}(1520)$  and small  $N(1440)P_{11}$  and  $D_{33}(1700)$  contributions. Our analysis finds a very strong  $D_{33}(1700)$  contribution. However, the dominant orbital angular momentum in the  $D_{33}(1700) \rightarrow \Delta\pi$  decay is ambiguous giving rise to two acceptable solutions. Both solutions are fully compatible with the  $D_{33}$   $\pi N$  elastic scattering amplitude (see Fig. 5 in [41]). The analysis presented here is constrained by a large number of data sets and exploits all two-particle correlations within the  $N\pi\pi$  final state. These technical differences may very well be a reason for the discrepant results.

The  $P_{11}$  amplitude for  $\pi N$  elastic scattering is written in the form of a K-matrix containing three constants, describing non-resonant contributions to elastic and inelastic reactions, and a series of poles representing resonant contributions. The  $P_{11}$  photoproduction amplitude is written as a K-matrix in

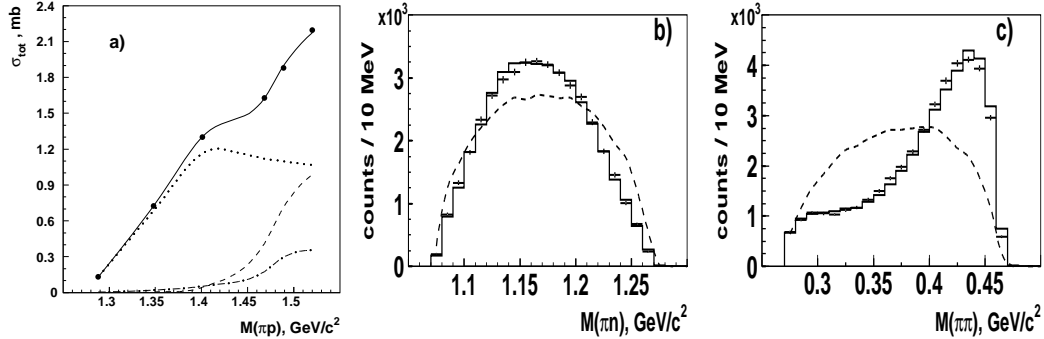


Fig. 7. The reaction  $\pi^- p \rightarrow n\pi^0\pi^0$  [47]. (a) Total cross section; the errors are smaller than the dots. (b)  $\pi^0 P$  and (c)  $\pi^0\pi^0$  invariant mass distributions for 551 MeV/c. In (a) the dotted, dashed and dashed dotted lines give the  $P_{11}$ ,  $D_{13}$ , and  $S_{11}$  contributions, respectively. In (b,c) data (crosses), fit (histogram) and phase space (dashed line) are shown. The distributions are not corrected for acceptance.

P-vector approach (which neglects  $p\gamma$  loops in the rescattering series). The photoproduction amplitude has the same poles as the scattering matrix. One constant each is introduced for reaction (1) and (2) in Table 1 describing direct  $p\pi^0$  and  $p\pi^0\pi^0$  production. The constants, pole positions and couplings  $g_{Nx}$  to a final state  $Nx$  are free parameters of the fit. The Born term is described by a pole at the proton mass. At least two poles were required, with pole positions at 1370 and 1850 MeV, respectively. In Fig. 6a,b we show the  $P_{11}$  amplitude for the two-pole solution. The data are well described.

As a next step, we introduced a second pole in the Roper region, a pion-induced resonance R and a second photo-induced R'. This attempt failed. The fit reduced the elastic width to the minimal allowed value of 50 MeV; the overall probability of the fit became unacceptable. The resulting elastic amplitude is shown in Fig. 6a,b as dashed line. We did not find any meaningful solution where the Roper region could comprise two resonances.

In [38,39], no evidence for  $N(1710)P_{11}$  was found. The increased sensitivity due to new data encouraged us to introduce a third pole in the  $P_{11}$  amplitude. Fig. 6c,d show the result of this fit. A small improvement due to  $N(1710)P_{11}$  is observed, and also other data sets are slightly better described. The parameters of the resonance are not well defined, the pole position is found in the 1580 to 1700 MeV mass range.

Introduction of the  $N(1710)P_{11}$  as third pole changes the  $N(1840)P_{11}$  properties. In the two-pole solution, the  $N(1840)P_{11}$  resonance is narrow ( $\sim 150$  MeV), in the three-pole solution, the  $N(1710)P_{11}$  and a  $\sim 250$  MeV wide  $N(1840)P_{11}$  resonance interfere to reproduce the structure. Data with polarized photons and protons will hopefully clarify existence and properties of these additional resonances. Further  $P_{11}$  poles are expected at larger masses. Introducing such a pole does not lead to a significant improvement of the fit.

Table 2

Properties of  $N(1440)P_{11}$ . The left column lists mass, width, partial widths of the Breit-Wigner resonance; the right column pole position and squared couplings to the final state at the pole position.

M	=	$1436 \pm 15$ MeV	$M_{\text{pole}}$	=	$1371 \pm 7$ MeV
$\Gamma$	=	$335 \pm 40$ MeV	$\Gamma_{\text{pole}}$	=	$192 \pm 20$ MeV
$\Gamma_{\pi N}$	=	$205 \pm 25$ MeV	$g_{\pi N}$	=	$(0.51 \pm 0.05) \cdot e^{-i\pi \frac{(35 \pm 5)}{180}}$
$\Gamma_{\sigma N}$	=	$71 \pm 17$ MeV	$g_{\sigma N}$	=	$(0.82 \pm 0.16) \cdot e^{-i\pi \frac{(20 \pm 13)}{180}}$
$\Gamma_{\pi \Delta}$	=	$59 \pm 15$ MeV	$g_{\pi \Delta}$	=	$(-0.57 \pm 0.08) \cdot e^{i\pi \frac{(25 \pm 20)}{180}}$
T-matrix:		$A_{1/2} = 0.055 \pm 0.020$ GeV	$\phi = (70 \pm 30)^\circ$		

The properties of the  $N(1440)P_{11}$  resonance determined here are listed in Table 2. From the K-matrix poles and their couplings, the poles of the scattering matrix T were deduced. The speed plot  $|dT|/dm$  gives  $M_{\text{speed}} \sim 1340$  MeV. The Breit-Wigner parameters are deduced by the following method. The helicity coupling and the coupling constant for a given decay mode are calculated as residues of the T-matrix pole in the corresponding complex  $s = M^2$  plane. These are complex numbers. The partial decay widths are calculated from the coupling constants and the available phase space including centrifugal barrier factor and Blatt-Weisskopf corrections [36]. These partial widths (including the missing width) are scaled by a common factor to reproduce the T-matrix pole position. The errors cover the range of a large variety of different PWA solutions.

The fractional yields of resonant and non-resonant parts are of course ill-defined quantities. To allow the reader to appreciate better the meaning of the results, we have set to zero the resonant or non-resonant part of the amplitude and calculated the corresponding cross sections, integrated over the Roper region (1300-1500 MeV). Interferences are neglected. The results on the different photoproduction reactions are presented in Table 3. Resonant and non-resonant contributions are comparatively large and interfere destructively to yield the observed  $P_{11}$  wave.

Table 3

Contributions of the  $P_{11}$ -wave to different photoproduction reactions, integrated over the 1300-1500 MeV mass range.

Reaction	$P_{11, \text{obs}}$ (%)	$P_{11, \text{res}}$ (%)	$P_{11, \text{nonres}}$ (%)
$\gamma p \rightarrow \pi^0 p$	$2.4 \pm 0.8$	$4 \pm 1$	$7 \pm 2$
$\gamma p \rightarrow \pi^0 \pi^0 p$	$7 \pm 2$	$6 \pm 2$	$11 \pm 3$
$\gamma p \rightarrow \Delta^+ \pi^0$	$5 \pm 1$	$4 \pm 1$	$7 \pm 2$
$\gamma p \rightarrow p \sigma$	$4 \pm 1$	$3 \pm 1$	$7 \pm 2$

Table 4

Fractional contributions (in %) of the  $N(1440)P_{11}$  and its isobars to  $\pi^- p \rightarrow p\pi^0\pi^0$  for 3 different  $\pi^-$  energies.

$p_\pi$ (MeV/c)	472	551	655
$\pi^- p \rightarrow P_{11} \rightarrow n\pi^0\pi^0$	$95 \pm 3$	$88 \pm 3$	$60 \pm 5$
$\pi^- p \rightarrow P_{11} \rightarrow \Delta^0\pi^0$	$22 \pm 3$	$29 \pm 3$	$25 \pm 3$
$\pi^- p \rightarrow P_{11} \rightarrow p\sigma$	$70 \pm 5$	$53 \pm 2$	$32 \pm 6$

This is different in pion scattering. The largest contribution to the  $n\pi^0\pi^0$  final state goes via the  $N(1440)P_{11}$  resonance. The complicated interference between resonant and non-resonant amplitudes may be the reason why the Roper resonance is so difficult to identify in photoproduction reactions.

The properties of the Roper derived here are mostly consistent with previous determinations. Pole position and Breit-Wigner mass and width fall into the range of values given by the Particle Data Group (PDG [1]),

$$M_{BW} = 1430 - 1470 \text{ MeV}; \quad \Gamma_{BW} = 250 - 450 \text{ MeV}$$

$$M_{\text{pole}} = 1345 - 1385 \text{ MeV}; \quad \Gamma_{\text{pole}} = 160 - 260 \text{ MeV}$$

but are defined more precisely here. The helicity coupling agrees with the PDG mean value but from the variety of different solutions we estimate a larger error. Note that our helicity amplitude is defined in the complex  $s = M^2$  plane at the pole position of the Roper. The elastic width ( $\Gamma_{N\pi}/\Gamma_{tot} = 0.612 \pm 0.020$ ) is compatible with previous findings (60-70%). Its decay fraction into  $\Delta\pi$  ( $\Gamma_{\Delta\pi}/\Gamma_{tot} = 0.176 \pm 0.020$ ) is not in conflict with the PDG mean value (20-30%); only the  $N\sigma$  partial decay width deviates significantly from PDG. We find  $\Gamma_{N\sigma}/\Gamma_{tot} = 0.212 \pm 0.030$  while PDG gives 5-10%.

Due to its larger phase space, decays into  $N\pi$  are more frequent than those into  $N\sigma$  even though the latter decay mode provides the largest coupling. For a radial excitation, this is not unexpected: about 50% of all  $\psi(2S)$  resonances decay into  $J/\psi\sigma$ , more than 25% of  $\Upsilon(2S)$  resonances decay via  $\Upsilon(1S)\sigma$  [1]. The large value of  $g_{\sigma N}$  might therefore support the interpretation of the Roper resonance as radial excitation.

An alternative interpretation of the  $N\pi\pi$  decay is offered by Hernandez, Oset and Vicente-Vacas [51] who take into account the re-scattering of the two final state pions. The authors of [51] do not fit data; instead they show that they can reproduce qualitatively the phenomenology of  $N(1440)P_{11} \rightarrow N\pi\pi$  decays by rescattering thus avoiding the need to introduce a genuine  $N(1440)P_{11} \rightarrow N\sigma$  amplitude.

In this letter, we have presented new data on photoproduction of two neutral pions in the energy range from the  $2\pi^0$  production threshold up to a photon energy of 820 MeV (Mainz) and up to 1300 MeV (Bonn) and reported results from a partial wave analysis of this and of related reactions.

The focus of this letter is the Roper resonance. We show that the data are incompatible with the conjecture that conflicting results on its properties could originate from the presence of two similar resonances and their interference, where both are in the  $P_{11}$  wave and both fall into the 1300 to 1500 MeV mass region. Due to the fact that the Roper properties are over-constrained by the data, we can rule out this possibility. The decay pattern is consistent with an interpretation of the Roper resonance as first radial excitation of the nucleon.

## Acknowledgements

We would like to thank the technical staff of the ELSA and MAMI machine groups and of all the participating institutions of their invaluable contributions to the success of the experiment. We acknowledge financial support from the Deutsche Forschungsgemeinschaft (DFG) within the SFB/TR16 and from the Schweizerische Nationalfond. The collaboration with St. Petersburg received funds from DFG and RFBR. U.Thoma thanks for an Emmy Noether grant from the DFG. A.V. Sarantsev acknowledges support from RSSF.

## References

- [1] W.M. Yao *et al.*, J. Phys. G **33** (2006) 1.
- [2] U.G. Meißner, J.W. Durso, Nucl. Phys. A **430** (1984) 670.
- [3] C. Hajduk, B. Schwesinger, Phys. Lett. B **140** (1984) 172.
- [4] S. Capstick, N. Isgur, Phys. Rev. D **34** (1986) 2809.
- [5] U. Löring *et al.*, Eur. Phys. J. A **10** (2001) 395.
- [6] U. Löring *et al.*, Eur. Phys. J. A **10** (2001) 447.
- [7] L.Y. Glozman *et al.*, Phys. Rev. D **58** (1998) 094030.
- [8] T. Burch *et al.*, Phys. Rev. D **74** (2006) 014504.
- [9] O. Krehl *et al.*, Phys. Rev. C **62** (2000) 025207.
- [10] S. Schneider *et al.*, Eur. Phys. J. A **28** (2006) 107.
- [11] Z.P. Li *et al.*, Phys. Rev. D **46** (1992) 70.

- [12] S. Capstick, P.R. Page, Phys. Rev. D **60** (1999) 111501.
- [13] T. Nakano *et al.*, Phys. Rev. Lett. **91** (2003) 012002.
- [14] V.V. Barmin *et al.*, Phys. Atom. Nucl. **66** (2003) 1715 [Yad. Fiz. **66** (2003) 1763].
- [15] S. Stepanyan *et al.*, Phys. Rev. Lett. **91** (2003) 252001.
- [16] J. Barth *et al.*, Phys. Lett. B **572** (2003) 127.
- [17] R.L. Jaffe and F. Wilczek, Phys. Rev. Lett. **91** (2003) 232003.
- [18] D. Diakonov *et al.*, Z. Phys. A **359** (1997) 305.
- [19] R. A. Arndt *et al.*, Phys. Rev. C **69** (2004) 035208.
- [20] M. Battaglieri *et al.*, Phys. Rev. Lett. **96** (2006) 042001.
- [21] S. Niccolai *et al.*, Phys. Rev. Lett. **97** (2006) 032001.
- [22] H.P. Morsch, P. Zupranski, Phys. Rev. C **61** (2000) 024002.
- [23] H. P. Morsch and P. Zupranski, Phys. Rev. C **71** (2005) 065203.
- [24] J. Patzold *et al.*, Phys. Rev. C **67** (2003) 052202.
- [25] J. Ahrens *et al.*, Nucl. Phys. News **4** (1994) 5.
- [26] W. Hillert, Eur. Phys. J. A **28S1** (2006) 139.
- [27] U. Thoma *et al.*, “ $N^*$  and  $\Delta^*$  decays into  $N\pi^0\pi^0$ ”, arXiv:0707.3592.
- [28] M. Kotulla *et al.*, Phys. Lett. B **578** (2004) 63.
- [29] F. Harter *et al.*, Phys. Lett. B **401** (1997) 229.
- [30] M. Wolf *et al.*, Eur. Phys. J. A **9** (2000) 5.
- [31] S.J. Hall *et al.*, Nucl. Instr. Meth. A **368** (1996) 698.
- [32] R. Novotny, IEEE Trans. Nucl. Sci. **38** (1991) 379.
- [33] A.R. Gabler *et al.*, Nucl. Instr. Meth. A **346** (1994) 168.
- [34] M. Kotulla *et al.*, Phys. Rev. Lett. **89** (2002) 272001.
- [35] Y. Assafiri *et al.*, Phys. Rev. Lett. **90** (2003) 222001.
- [36] A.V. Anisovich *et al.*, Eur. Phys. J. A **24** (2005) 111.
- [37] A.V. Anisovich and A.V. Sarantsev, Eur. Phys. J. A **30** (2006) 427.
- [38] A.V. Anisovich *et al.*, Eur. Phys. J. A **25** (2005) 427.
- [39] A.V. Sarantsev *et al.*, Eur. Phys. J. A **25** (2005) 441.

- [40] A.V. Anisovich *et al.*, “Baryon resonances and polarization transfer in hyperon photoproduction”, arXiv:0707.3596.
- [41] I. Horn *et al.*, “Evidence for two negative-parity  $\Delta D_{33}$  excitations decaying into  $\Delta\eta$ ”, in preparation.
- [42] O. Bartholomy *et al.*, Phys. Rev. Lett. **94** (2005) 012003.
- [43] H. van Pee *et al.*, Eur. Phys. J. A **31** (2007) 61.
- [44] O. Bartalini *et al.*, Eur. Phys. J. A **26** (2005) 399.
- [45] M. Dugger *et al.*, Phys. Rev. C **76** (2007) 025211.
- [46] R. A. Arndt *et al.*, Phys. Rev. C **74** (2006) 045205.
- [47] S. Prakhov *et al.*, Phys. Rev. C **69** (2004) 045202.
- [48] R.A. Arndt *et al.*, <http://gwdac.phys.gwu.edu>.
- [49] J.A. Gomez Tejedor and E. Oset, Nucl. Phys. A **600** (1996) 413.
- [50] J.C. Nacher *et al.*, Nucl. Phys. A **695** (2001) 295.
- [51] E. Hernandez, E. Oset and M. J. Vicente Vacas, Phys. Rev. C **66**, (2002) 065201.